Geomorphology 328 (2019) 231–237

Contents lists available at ScienceDirect

Geomorphology

journal homepage: www.elsevier.com/locate/geomorph

Comment on 'Geophysical approach to the study of a periglacial blockfield in a mountain area (Ztracené kameny, Eastern Sudetes, Czech Republic)' by Stan et al. (2017)

Tomáš Uxa [a,b,*], Marek Křížek [a], David Krause [a], Filip Hartvich [a,c], Petr Tábořík [d,c], Marek Kasprzak [e]

[a] Department of Physical Geography and Geoecology, Faculty of Science, Charles University, Albertov 6, 128 43 Prague 2, Czech Republic
[b] Institute of Geophysics, Czech Academy of Sciences, Boční II 1401, 141 31 Prague, 4, Czech Republic
[c] Institute of Rock Structure and Mechanics, Czech Academy of Sciences, V Holešovičkách 41, 182 09 Prague, 8, Czech Republic
[d] Institute of Hydrogeology, Engineering Geology and Applied Geophysics, Faculty of Science, Charles University, Albertov 6, 128 43 Prague 2, Czech Republic
[e] Department of Geomorphology, Institute of Geography and Regional Development, University of Wrocław, pl. Uniwersytecki 1, 50-137 Wrocław, Poland

ARTICLE INFO

Article history:
Received 3 July 2018
Received in revised form 10 October 2018
Accepted 10 October 2018
Available online 13 October 2018

Keywords:
Blockfield
Permafrost
Electrical resistivity tomography
Seismic refraction tomography
Eastern High Sudetes
Central Europe

ABSTRACT

Stan et al. (2017) investigated the internal structure of two periglacial blockfields on the Ztracené kameny site, Eastern High Sudetes, Czech Republic, using electrical resistivity tomography and seismic refraction tomography and interpreted two high-resistivity and high-velocity zones as remnants of the Pleistocene permafrost. However, we believe that in reality no permafrost occurs on the site, and we provide alternate, non-permafrost interpretations of the geophysical measurements by Stan et al. (2017) that are well consistent with other evidences such as climate and topographic attributes of the blockfields, permafrost-disqualifying ground thermal regimes, and common characteristics of mid-latitude, low-altitude permafrost locations from elsewhere. We also rectify some misconceptions about the study site that are stated by Stan et al. (2017).

1. Introduction

Openwork debris of blockfields, talus slopes, or rock glaciers permits the air to flow through the pore spaces and to develop a seasonally reversing, gravity-driven internal air circulation. This convective heat transfer induces inhomogeneous temperature distribution across the scree slopes; with up to several degrees Celsius cooler air in their lower parts. The latter places frequently show notable negative thermal anomalies, which are essential for potential maintenance of subzero mean annual ground temperature (MAGT) even if mean annual air temperature (MAAT) is well above zero (e.g., Delaloye and Lambiel 2005; Wicky and Hauck 2017). The difference between MAGT and MAAT is mostly a few degrees Celsius below zero (e.g., Delaloye et al. 2003; Gorbunov et al. 2004), but it can achieve −5 °C or less (e.g., Zacharda et al. 2007; Morard et al. 2010; Popescu et al. 2017). Consequently, scree slopes are capable to host perennial ice patches in surprisingly low altitudes and otherwise permafrost-free environments (Table 1). Such locations are therefore of high interest for permafrost researchers as well as for biologists because these azonal permafrost spots are abundantly colonized by boreo-alpine flora and fauna species characteristic of much higher altitudes or latitudes, which can even be relics from glacial periods (e.g., Gude et al. 2003; Stiegler et al. 2014). However, controls on permafrost occurrence in such specific places and anomalous regional environmental conditions as well as their state under a changing climate are still little understood as these locations are very scarce (Table 1). Each new report is therefore of high scientific importance and worthy of attention and should be properly documented as it can alter our understanding of azonal permafrost occurrence. Such a report is also the recently published study of Stan et al. (2017) aimed at a shallow geophysical survey of the internal structure of two periglacial blockfields on the Ztracené kameny (1250 m asl), Eastern High Sudetes, Czech Republic, utilizing electrical resistivity tomography (ERT) and seismic refraction tomography (SRT; commonly called 'shallow seismic refraction'), in which the authors interpreted two isolated high-resistivity and high-velocity zones as permafrost patches that were, moreover, thought to be of Pleistocene age. We have serious doubts about the validity of the purely geophysically suggested contemporary permafrost occurrence on the Ztracené kameny by Stan et al. (2017) because we consider their interpretation of the ERT and SRT measurements to be oversimplifying and unilaterally favouring the

* Corresponding author at: Department of Physical Geography and Geoecology, Faculty of Science, Charles University, Albertov 6, 128 43 Prague 2, Czech Republic.
E-mail address: tomas.uxa@natur.cuni.cz (T. Uxa).

https://doi.org/10.1016/j.geomorph.2018.10.010
0169-555X/

Table 1
Characteristics of the geophysically prospected mid-latitude, low-altitude permafrost sites in Europe.

Country	Switzerland	France	Germany	Germany	Switzerland	Germany	Austria	Czech Republic	Czech Republic	Romania
Location	Creux-du-Van Jura Mts.	La Glacière Vosges Mts.	Präg Schwarzwald Mts.	Zastler Schwarzwald Mts.	Val Bever Swiss Alps	Odertal Harz Mts.	Toteisboden Schladminger Tauern Range	Kamená hůra Central Bohemian Highlands	Klíč Central Bohemian Highlands	Detunata Goală Apuseni Mts.
Landform	Talus slope	Scree slope	Scree slope	Scree slope	Scree slope	Talus slope -moraine	Talus slope	Talus slope	Talus slope	Talus slope-rock glacier
Longitude	6°44′ E	6°58′ E	7°58′ E	8°00′ E	9°51′ E	10°33′ E	13°42′ E	14°21′ E	14°34′ E	23°12′ E
Latitude	46°56′ N	48°06′ N	47°47′ N	47°55′ N	46°33′ N	51°44′ N	47°21′ N	50°42′ N	50°47′ N	46°17′ N
Altitude (m)	1170–1300	680	720	590	1790–1900	600	990–1040	300–360	520–600	1020–1110
Vertical range (m)	130	–	–	–	110	–	50	60	80	90
Aspect	N	–	–	–	N	W	N	N	SW	W
MAAT (°C)	5.4	–	–	–	1	6.2	4.7	8	7.1	8.4
MAGT in the lower part (°C)	0.7 to 3.3	–	–	–	−0.9	1.6	−0.8	−0.9	0.4	1.0–2.6
Temperature offset (°C)	−4.7 to −2.1	–	–	–	−1.9[a]	−4.6	−5.5[a]	−8.9	−6.7	−7.4 to −5.8
Resistivity (kΩ·m)	5–37	<100	<100	<100	>20 to 60–140	–	30–50 to 200	–	>360	20–65
P-wave velocity ($m\cdot s^{-1}$)	–	<2000	<2000	<2000	1700–4300	2500–3500	>1500	<1000	2000–3000	–
Scree thickness (m)	20	–	10?	10?	>11–23	>15	>6–25	10–15	15–20	>10–25
Active-layer thickness (m)	2–3	1–5	–	–	1–3	–	1–5	–	2–5	4–9
Permafrost thickness (m)	15–20	ca. 5	<10	<10	10–20	–	5–20	–	<2	6–16
Lower limit of discontinuous permafrost (m)	2200–2400	–	–	–	2400	–	2400	–	–	–
Lithology	Limestone	–	–	–	–	–	Granite-gneiss	Olivine basalt	Phonolite	Basaltic andesite
Vegetation	Organic soil and patches of dwarf red spruce in the lower part	Sparse vegetation	Sparse vegetation	Sparse vegetation	Small larch trees	–	Mosses and cryophilic plants with isolated spots of dwarf birch	Dense cover of non-vascular plants in the lower part	Lichens and mosses in the lower part	Mosses and dwarf trees in the lower part
Source	Delaloye et al. (2003) Morard et al. (2008)	Hauck and Kneisel (2008)	Hauck and Kneisel (2008)	Hauck and Kneisel (2008)	Kneisel et al. (2000) Kneisel (2010)	Gude et al. (2003) Růžička et al. (2015)	Stiegler et al. (2014)	Gude et al. (2003) Zacharda et al. (2005) Růžička et al. (2015)	Gude et al. (2003) Zacharda et al. (2005) Růžička et al. (2015)	Popescu et al. (2017)

[a] Temperature offset calculation based on the long-term MAAT.

presence of permafrost although the local conditions are highly disadvantageous for its existence.

In this comment, we propose an alternate explanation of these ambiguous geophysical data sets and provide other considerations, which lead us to believe that no buried perennial ground ice actually exists there.

2. Geophysical outputs and their reinterpretation

Shallow geophysical techniques, such as ERT and SRT, have been widely employed in mid-latitude, low-altitude permafrost detection (e.g., Kneisel et al. 2000; Delaloye et al. 2003; Gude et al. 2003; Hauck and Kneisel 2008; Stiegler et al. 2014; Popescu et al. 2017) because ice and ice-rich sediments show high electrical resistivities (ca. 10^3–10^6 $\Omega\cdot$m) and high P-wave velocities (ca. 1500–5300 m.s^{-1} and mostly ca. 2000–4000 m$\cdot$s^{-1}), which commonly contrast well with those of the surrounding materials (Kneisel and Hauck 2008; Schrott and Hoffmann 2008; Schrott and Sass 2008; Draebing 2016). Both methods are therefore extremely useful for localizing and quantifying ground-ice bodies, especially when combined; but in no case have they been applied to mid-latitude, low-altitude permafrost exploration independently of other, mostly temperature-based methods (air and ground temperature monitoring, mapping of the bottom temperature of snow cover, spring-water temperature measurements, infrared imaging; e.g., Kneisel et al. 2000; Delaloye et al. 2003; Gude et al. 2003; Stiegler et al. 2014; Popescu et al. 2017) because influences that can make their interpretation difficult are numerous (Draebing 2016). The characteristic values of electrical resistivity and P-wave velocity usually considered for ice-bearing materials in mid-latitude, low-altitude locations are rather low and range between ca. 5–50 k$\Omega\cdot$m and <100 k$\Omega\cdot$m (e.g., Kneisel et al. 2000; Delaloye et al. 2003; Stiegler et al. 2014; Popescu et al. 2017) and 2000–3500 m$\cdot$s^{-1} respectively (e.g., Kneisel et al. 2000; Gude et al. 2003) because permafrost at most of these places is assumed to be warm, with temperatures close to 0 °C and low ice contents or high unfrozen water contents (Kneisel et al. 2000). The resistivities around 100 k$\Omega\cdot$m and higher are commonly assigned to large ice-coated boulders with air-filled voids (e.g., Kneisel et al. 2000; Stiegler et al. 2014) rather than to massive ice bodies that are typical for high-alpine environments (Hauck and Vonder Mühll 2003). Furthermore, P-wave velocities of 2500–3500 m$\cdot$s^{-1} can indicate the occurrence of ice as well as the presence of bedrock (Gude et al. 2003).

Stan et al. (2017) identified an isolated zone of high resistivities well over 100 k$\Omega\cdot$m (up to ca. 200 k$\Omega\cdot$m) at an average depth of ca. 6 m (depth range of ca. 4–8 m) on their ERT profile E1, located in the lower part of the 'eastern' blockfield, which spatially coincides with the zone of high P-wave velocities of up to 3000 m$\cdot$s^{-1} on the SRT profile E3, perpendicularly intersecting the profile E1 (see Fig. 7 in Stan et al. 2017, p. 384). Similarly, an isolated zone of high resistivities over 80 k$\Omega\cdot$m at an average depth of ca. 5.5 m (depth range of ca. 2–7 m) was recorded on their ERT profile W6, located in the lower part of the 'western' blockfield, which corresponds with the zone of high P-wave velocities of up to 2000 m$\cdot$s^{-1} on the SRT profile W3, transversally crossing the profile W6 (see Fig. 11 in Stan et al. 2017, p. 387). Both these high-resistivity and high-velocity zones were interpreted by Stan et al. (2017) as the remnants of probably Pleistocene permafrost.

Generally, some of the electrical resistivity values measured by Stan et al. (2017) on the Ztracené kameny may suggest the presence of permafrost as they largely overlap the entire interval of resistivities that are characteristic of ice and ice-rich sediments (see above). On the contrary, the maximum resistivities mostly attain or even exceed the highest values documented from mid-latitude, low-altitude permafrost sites (cf. Kneisel et al. 2000; Delaloye et al. 2003; Gude et al. 2003; Stiegler et al. 2014; Popescu et al. 2017), rather resembling the massive ice (sensu Hauck and Vonder Mühll 2003). However, the resistivities of up to ca. 200 k$\Omega\cdot$m recorded within the 'eastern' blockfield are probably too large to be produced by ground ice alone in this permafrost-hostile environment (see Section 3), and thus a certain share of ice-free voids would likely be needed to generate such extreme values (sensu Kneisel et al. 2000; Stiegler et al. 2014). Nonetheless, the P-wave velocities of up to 3000 m$\cdot$s^{-1} measured in the same place unambiguously exclude a larger presence of air as it itself achieves values as low as 300–330 m.s^{-1} and the typical values for air-filled layers commonly show the left-skewed range of ca. 350–1500 m$\cdot$s^{-1} (Draebing 2016), which, in fact, includes almost the entire velocity span of ca. 250–1200 m$\cdot$s^{-1} observed by Stan et al. (2017) in these substrates. Likewise, the maximum resistivities over 80 kΩ.m measured within the 'western' blockfield would presumably also need the presence of air-filled voids to attain such high values, but the P-wave velocities of this lenticular structure are up to 2000 m$\cdot$s^{-1}, which almost certainly excludes the presence of air and ice (cf. Kneisel et al. 2000; Gude et al. 2003; Schrott and Hoffmann 2008; Draebing 2016). Because the existence of large amounts of perennial ice is highly improbable in this altitude (ca. 1100–1250 m asl) and the presence of air-ice mixture can be declined as well (sensu Kneisel et al. 2000; Stiegler et al. 2014), the high-resistivity and high-velocity zones can hardly be interpreted as permafrost lenses. Notably, Stan et al. (2017) also measured comparably high electrical resistivities in other parts of their ERT profiles E1 and W6 as well as P1 (see Figs. 6, 7, and 11 in Stan et al. 2017, pp. 384 and 387), which locally have even larger spatial extents than the two 'permafrost' patches; but surprisingly, these zones attracted substantially less attention of Stan et al. (2017), and if so, they were mostly interpreted as loosely packed blockfield with air-filled voids.

Our alternate explanation for such widespread occurrence of the extreme resistivities on the Ztracené kameny is that both blockfields are composed of a mixture of Palaeozoic metamorphic rocks, with a dominance of quartzites. High quartz content of rocks (see the right photograph on Fig. 3 and Fig. 1 in Stan et al. 2017, p. 381) is certainly able to produce very high electrical resistivities because quartzites show a huge range of values between 10 and 10^9 $\Omega\cdot$m (Kneisel and Hauck 2008) and pure quartz even well above 10^{10} $\Omega\cdot$m (e.g., Parkhomenko 1967; Telford et al. 1990). Consequently, the high-resistivity zones can be associated with the occurrences of solid quartzite bedrock, larger quartzite boulders, quartz veins traversing the blockfields, or locally increased quartz content. The ERT profile E1 (see Fig. 7 in Stan et al. 2017, p. 384) transversally intersects the assumed quartzite insertions or veins (Stan et al. 2017), running roughly in the NE-SW direction (Fig. 1), the most compact sections of which probably achieve the highest resistivities over ca. 70 k$\Omega\cdot$m, while their disrupted parts exhibit somewhat lower values of ca. >20 k$\Omega\cdot$m. This layer is superposed by packed blocks with voids filled by organics and other fine materials (Stan et al. 2017, p. 385) as well as by air, which reach an average depth of ca. 4 m and are characterized by resistivities and P-wave velocities less than ca. 20 k$\Omega\cdot$m and ca. 1200 m$\cdot$s^{-1} respectively. The high-resistivity zone (>80 k$\Omega\cdot$m) on the ERT profile W6 (see Fig. 11 in Stan et al. 2017, p. 387) could be attributed to the presence of a large isolated boulder with high quartz content, which is set inside the less resistive environment composed of smaller blocks with void-filling organics and fine materials, which also have the resistivities lower than ca. 20 k$\Omega\cdot$m and P-wave velocities ca. 1200 m$\cdot$s^{-1} as in the 'eastern' blockfield. The comparably high resistivities in the ca. 3 m thick uppermost layer, located in the entire above-lying part of profile W6, are likely caused by a block cover with air-filled voids. The high resistivity (ca. >20 k$\Omega\cdot$m) in the SW section of ERT profile P1 (see Fig. 6 in Stan et al. 2017, p. 384) is related to shallow or exposed bedrock around and on the top rock formation of the Ztracené kameny as actually stated by Stan et al. (2017) as well.

The blockfields probably tend to increase their thickness downslope because the ERT profiles E4, E5, W7, W8, and W9 (see Figs. 8, 12, and 13 in Stan et al. 2017, pp. 385, 387, and 388), situated in the lower-lying densely forested areas, show the uppermost layer of ca. 10–15 m with resistivity <20 k$\Omega\cdot$m, which is probably composed of highly weathered quartzite blocks and voids completely filled with fine material. This layer likely corresponds to the second layer identified in the

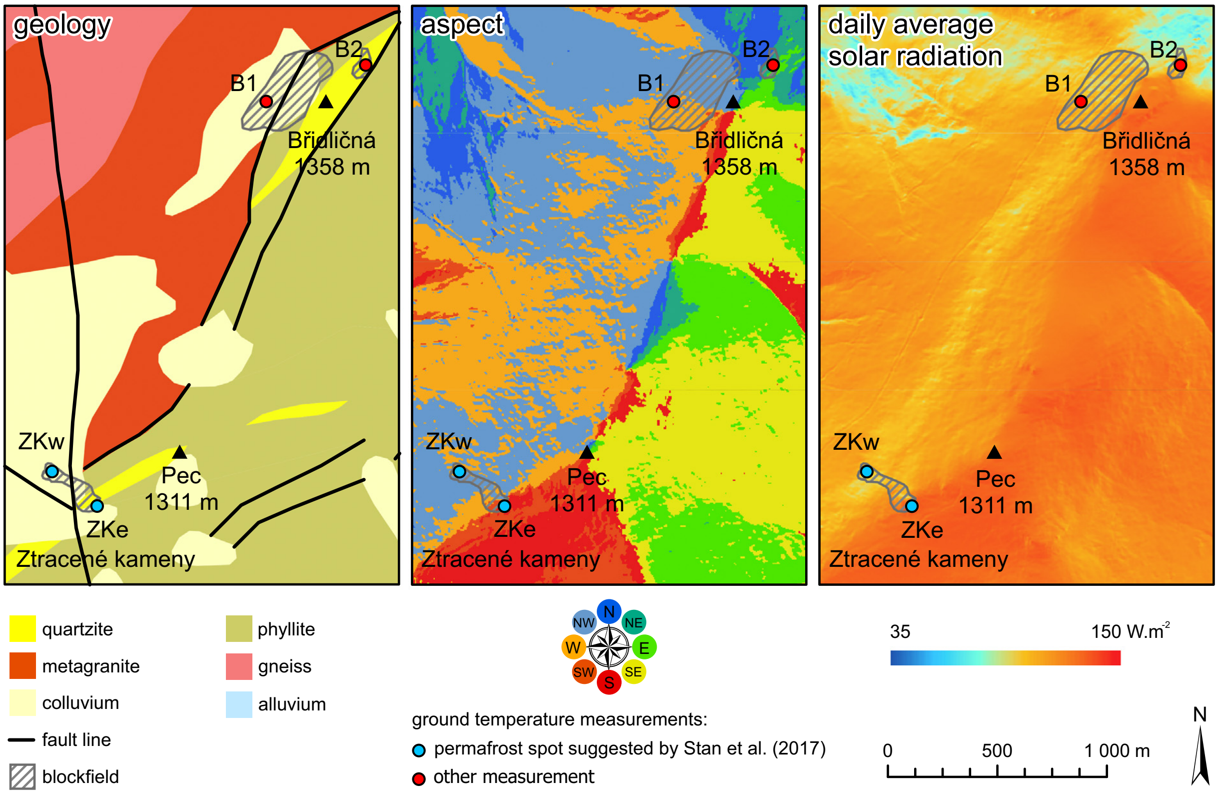

Fig. 1. Geology, aspect, and solar radiation in the study area. ZKw – permafrost spot suggested by Stan et al. (2017) on the 'western' blockfield on the Ztracené kameny; ZKe – permafrost spot suggested by Stan et al. (2017) on the 'eastern' blockfield on the Ztracené kameny; B1 – ground temperature measurement site on the Mt. Břidličná blockfield 1; B2 – ground temperature measurement site on the Mt. Břidličná blockfield 2.

unvegetated parts of the blockfields as both have very similar resistivities. The latter, however, extends to smaller depth as most ERT and SRT profiles in the forest-free parts of the blockfields suggest the bedrock occurrence at ca. 8–12 m (see Figs. 6, 7, 9, 10, and 11 in Stan et al. 2017, pp. 384, 386, and 387).

3. A brief insight into permafrost history and present-day environmental setting

Undoubtedly, permafrost existed in the Eastern High Sudetes and their lower-elevated surroundings during the last glacial period based on the presence of permafrost-related landforms, such as cryoplanation terraces, blockfields and block streams, or large-scale sorted patterned ground (e.g., Křížek 2016), and according to the subsurface ground temperature history (Šafanda and Rajver 2001). It surely occupied this region particularly during the Last Glacial Maximum (26.5–19 ka BP) or the Last Permafrost Maximum (25–17 ka BP) respectively (Vandenberghe et al. 2014; Lindgren et al. 2016) when its modelled maximum thickness was up to 220–245 m in the summit area (Czudek 1986). Permafrost began to decay at the Pleistocene-Holocene transition when the ground surface temperature rose above 0 °C (Šafanda and Rajver 2001), and it is believed to completely disappear until the middle Holocene (Czudek 1986, 1997). This probably coincides with the period of somewhat higher regional MAAT than at present as suggested by numerous evidence (e.g., Šafanda and Rajver 2001; Rybníček and Rybníčková 2004; Dudová et al. 2013). However, Stan et al. (2017) still argued that the blockfields on the Ztracené kameny have favourable topoclimatic conditions for the permafrost preservation because they (i) have concave topography around the high-resistivity zones, (ii) are colder, (iii) have long-lasting insulating snow cover, (iv) are shaded, (v) lie on the edge of a forest, and (vi) have limited thermal insulation (Stan et al. 2017, pp. 387–388). Except for the last point, which is nonsensical by nature because it in itself excludes the persistence of perennial ice under the positive MAAT and also largely contradicts point (iii), we address the remaining statements thoroughly in the next paragraph.

Stan et al. (2017, p. 381) stated that the MAAT in the 'summit areas' of the Eastern High Sudetes is as low as 1.1 °C. However, the MAAT at Mt. Praděd (1491 m asl; the highest peak of the mountain range) and at Mt. Šerák (1328 m asl), located ca. 8.5 km and ca. 19.7 km from the Ztracené kameny respectively in 1985–1996 and 2004–2017 was 1.3 °C and 3.4 °C respectively (Jeseníky Protected Landscape Area authority; National Oceanic and Atmospheric Administration Climate Data Online). The MAAT in the study area (1100–1250 m asl) is therefore likely to be 2.9–4.9 °C if the standard air temperature lapse rate of 0.0065 $K \cdot m^{-1}$ is considered. This could facilitate potential permafrost maintenance if temperature offset is sufficient. Nonetheless, the mean ground temperature recorded directly at the suggested permafrost spots (Fig. 1) in the 'western' and 'eastern' blockfield between 25 May 2017 and 18 May 2018 at a depth of ca. 0.40 m and ca. 0.55 m below ground surface respectively was as high as 5.3 °C and 4.8 °C respectively, which was ca. 0.8 °C and ca. 0.9 °C above the mean air temperature estimated based on data from the Mt. Šerák station respectively (Fig. 2). Likewise, the ground temperatures had reached their absolute minima of −7.1 °C and −7.5 °C respectively before the snow cover established at the turn of November–December and, except of some cooling events caused by rapid drops of air temperature, they remained mostly above −2 °C throughout the winter (Fig. 2). This evidence alone almost totally excludes the presence of permafrost on the Ztracené kameny. Moreover, the MAGTs measured at mid-latitude, low-altitude permafrost sites were substantially lower, and importantly, none of these locations showed a positive temperature offset (Table 1). In fact, most mid-latitude, low-altitude permafrost occurrences have been reported particularly from north-, east-, or west-facing debris-covered sites (Table 1), which are colder than south-facing slopes because of limited sunshine duration (Kneisel et al. 2000; Gorbunov et al. 2004). Furthermore, these permafrost-prone debris accumulations commonly have

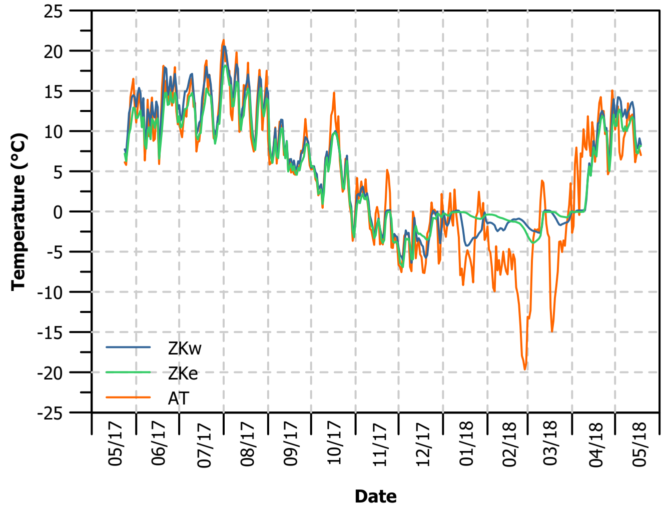

Fig. 2. Mean daily ground temperatures measured at the 'western' (ZKw) and 'eastern' (ZKe) permafrost spot suggested by Stan et al. (2017) within the blockfields on the Ztracené kameny and mean daily air temperature (AT) estimated for their average altitude based on data from the Mt. Šerák station and the standard air temperature lapse rate of 0.0065 $K \cdot m^{-1}$.

Fig. 3. The 'eastern' blockfield on the Ztracené kameny on 16 February 2017 when snow cover culminated (upper) and the same site on 30 October 2010 without snow (lower). On the left photograph, note the boulders sticking out of the relatively thin snow cover, with only the smallest blocks covered completely.

the elevation extent of higher tens or even hundreds of meters and are at least 10–15 m thick (Table 1), which allows air circulation to fully develop and also isolates the ice body from warmer ambient air temperatures because of the enhanced temperature offset (sensu Gorbunov et al. 2004). Thicker screes also accumulate larger amounts of ice in winter, which are then able to persist throughout the summer (Delaloye et al. 2003). Importantly, the blockfields surveyed by Stan et al. (2017) are titled based on their relative position to the top rock formation, but in reality, the 'western' and 'eastern' blockfields face to the northwest (298°) and south (193°) respectively (Fig. 1; see also Figs. 3 and 4 in Stan et al. 2017, pp. 382 and 383). This causes a high solar radiation input particularly to the south-oriented blockfield, which is, moreover, only partly shaded by trees (Fig. 1; cf. Stan et al. 2017, p. 387). Symptomatic of rather warm and dry conditions within both blockfields is also the absence of a denser vegetation cover consisting of mosses and cryophilic plants, which are frequently found in most mid-latitude, low-altitude permafrost sites (e.g., Delaloye et al. 2003; Gude et al. 2003; Zacharda et al. 2007; Stiegler et al. 2014; Popescu et al. 2017). Instead, the blockfields host scattered dwarf shrubs or trees spreading from the neighbouring forest, the dead organics of which fills the interior voids together with other fine materials (see Stan et al. 2017, p. 385), and thus prevents the air circulation. Furthermore, the 100–200 cm maximum thickness of up to six months lasting snow cover stated by Stan et al. (2017, p. 381) can well occur particularly on the leeward sides of the summit plateaus (Jeník 1961). However, the Ztracené kameny site is situated a little lower, below the alpine timberline, implying that somewhat thinner snowpack is to be expected there. Indeed, the snow is usually not thick enough to cover the blockfields continuously (Fig. 3) throughout the winter and mostly completely disappears in March–April, and then the ground temperature rises sharply (Fig. 2). Therefore, the blockfields are insulated over a limited part of the year, and even during this period the insulation is debatable because air can penetrate easily around the boulders protruding from the snow. Moreover, it is unclear whether this amount of snow can accumulate sufficient volumes of ice that could survive to the following winter (sensu Delaloye et al. 2003). Finally, both blockfields have rather low elevation extent of ca. 65 m (lower, uninterrupted part of the 'western' blockfield) and ca. 20 m respectively, are relatively shallow with bedrock depth in forest-free parts commonly up to ca. 8–12 m (as can be seen on most ERT and SRT profiles; see Figs. 6, 7, 9, 10, and 11 in Stan et al. 2017, pp. 384, 386, and 387), and have relatively straight slopes with no distinct concave areas around the suggested permafrost spots (Fig. 4) described by Stan et al. (2017, p. 387). This likely considerably reduces the potential for internal air circulation and formation of cold reservoirs in lower parts of the blockfields (sensu Delaloye et al. 2003; Delaloye and Lambiel 2005; Morard et al. 2008, 2010; Popescu et al. 2017). Consequently, in summary, the environmental setting of the Ztracené kameny is probably unable to host permafrost under the present-day climate conditions. This statement is also supported by the ground thermal regimes in the lower parts of two blockfields of the same geology, located on the northwestern and northeastern slopes of Mt. Břidličná (1358 m asl) ca. 2 km north of the Ztracené kameny (Fig. 1), which showed permafrost-disfavouring MAGT of 4.1 °C and 5.0 °C respectively in 2014 (Křížek, unpublished data from temperature dataloggers) when Stan et al. (2017) performed their geophysical survey. If we consider that the blockfields at Mt. Břidličná are potentially more suitable for permafrost occurrence because they have lower estimated MAAT (2.5–3.6 °C), receive equal or less solar radiation (daily average of 111 and 110 $W \cdot m^{-2}$ for Mt. Břidličná vs. 107 and 141 $W \cdot m^{-2}$ for the 'western' and 'eastern' blockfields on the Ztracené kameny; Fig. 1), and are larger and thicker than those on the Ztracené kameny as well, then the permafrost suggestions of Stan et al. (2017) seem even more dubious.

The above implies that permafrost could not exist on the Ztracené kameny in the middle Holocene as well (cf. Czudek 1986, 1997) when MAAT was up to 3 °C higher than at present (Rybníček and Rybníčková 2004; Czudek 2005; Dudová et al. 2013) and also when the precipitation totals were higher, and thus larger amounts of water could enter the blockfields and supply additional heat for potential ice melting. Moreover, the blockfields probably had more extensive vegetation and soil cover, which filled the interior voids, and thus further

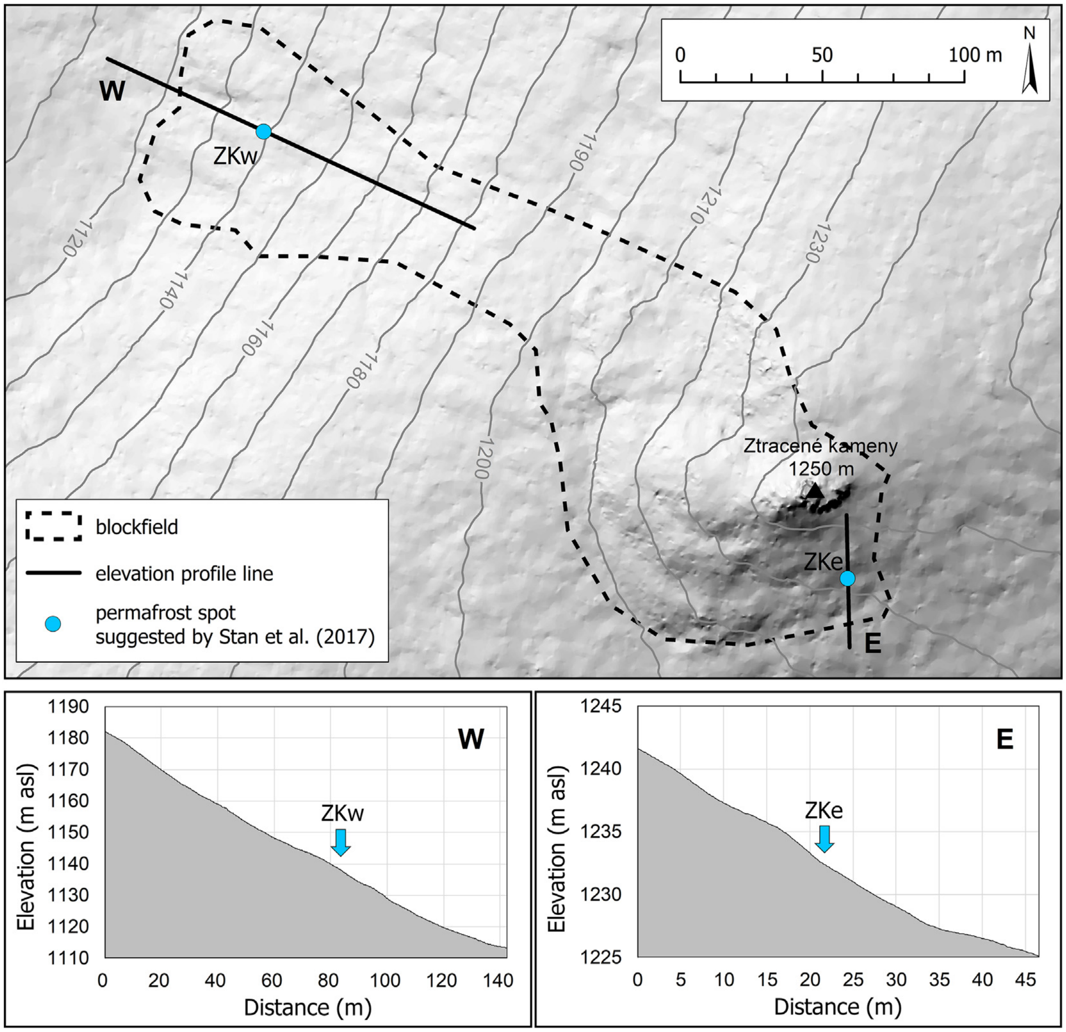

Fig. 4. Longitudinal elevation profiles across the 'western' (W) and 'eastern' (E) blockfields on the Ztracené kameny based on the 1 m DEM (State Administration of Land Surveying and Cadastre, 2017) with highlighted positions of the permafrost spots (ZKw and ZKe) suggested by Stan et al. (2017). Note that both spots are located on straight slopes.

reduced the potential for permafrost preservation. Consequently, even if present, the alleged ground-ice patches could hardly be termed as the remnants of Pleistocene permafrost as stated by Stan et al. (2017) because it thawed in the meantime (i.e., in the middle Holocene). Such shallow and tiny permafrost bodies are impacted by year-to-year air temperature variations, and thus they must exist under more-or-less equilibrium with contemporary climate otherwise they disappear. True relict permafrost reflects a colder past climate and is usually situated tens to hundreds of meters beneath the ground surface (e.g., Szewczyk and Nawrocki 2011) where it persists until the positive temperatures propagate into its depth level.

4. Conclusions

The contemporary permafrost existence in the two blockfields on the Ztracené kameny unilaterally proposed by Stan et al. (2017) is of doubtful validity as it relies on ambiguous geophysical data sets alone, poorly supported by other evidence. Maximum resistivity and P-wave velocity values should be attributed to the presence of high-resistivity quartzites and loose debris with air-filled voids, which produce geophysical images mimicking the permafrost conditions. The latter, non-permafrost hypothesis is also favoured by numerous evidence, such as the disadvantageous climate and topographic attributes of the blockfields, permafrost-disqualifying ground thermal regimes on the Ztracené kameny and in nearby blockfields, and common characteristics of mid-latitude, low-altitude permafrost locations from elsewhere, which all suggest it is highly improbable that the blockfields on the Ztracené kameny contain permafrost under the present climate.

Finally, we emphasize that geophysics delivers only indirect information with an artificial visualisation of the approximate subsurface distribution of physical parameters, which includes the ambiguity of the computed model and of the interpretation. Geophysical surveying therefore requires other non-geophysical inputs and a good knowledge of local conditions to support the hypothesized explanation as can be ultimately exemplified in most earlier mid-latitude, low-altitude permafrost investigations (e.g., Kneisel et al. 2000; Delaloye et al. 2003; Gude et al. 2003; Stiegler et al. 2014; Popescu et al. 2017). If no such information is available, then the reliable interpretation is almost impossible (Schrott and Sass 2008).

Declarations of interest

None.

Acknowledgements

We would like to thank two anonymous reviewers for their constructive comments, and the Editor-in-Chief, Richard A. Marston, for final editing of the paper. This work was supported by the Czech Science Foundation (grant number 17-21612S) and the Center for Geosphere Dynamics (grant number UNCE/SCI/006).

Appendix A. Supplementary data

Supplementary data associated with this article can be found in the online version at doi:https://doi.org/10.1016/j.geomorph.2018.10.010. These data include the Google map of the most important areas described in this article.

References

Czudek, T., 1986. Pleistocénní permafrost na území Československa. Geografický časopis 38, 245–252.

Czudek, T., 1997. Reliéf Moravy a Slezska v kvartéru. Sursum, Tišnov.

Czudek, T., 2005. Vývoj reliéfu krajiny České republiky v kvartéru. Moravské zemské muzeum, Brno.

Delaloye, R., Lambiel, C., 2005. Evidence of winter ascending air circulation throughout talus slopes and rock glaciers situated in the lower belt of alpine discontinuous permafrost (Swiss Alps). Nor. Geol. Tidsskr. 59, 194–203. https://doi.org/10.1080/00291950510020673.

Delaloye, R., Reynard, E., Lambiel, C., Marescot, L., Monnet, R., 2003. Thermal anomaly in a cold scree slope (Creux du Van, Switzerland). In: Phillips, M., Springman, S.M., Arenson, L.U. (Eds.), Proceedings of the 8th International Conference on Permafrost. Zurich, Switzerland, pp. 175–180.

Draebing, D., 2016. Application of refraction seismics in alpine permafrost studies: A review. Earth Sci. Rev. 155, 136–152. https://doi.org/10.1016/j.earscirev.2016.02.006.

Dudová, L., Hájková, P., Buchtová, H., Opravilová, V., 2013. Formation, succession and landscape history of Central-European summit raised bogs: A multiproxy study from the Hrubý Jeseník Mountains. The Holocene 23, 230–242. https://doi.org/10.1177/0959683612455540.

Gorbunov, A.P., Marchenko, S.S., Seversky, E.V., 2004. The Thermal Environment of Blocky Materials in the Mountains of Central Asia. Permafr. Periglac. Process. 15, 95–98. https://doi.org/10.1002/ppp.478.

Gude, M., Dietrich, S., Mäusbacher, R., Hauck, C., Molenda, R., Ruzicka, V., Zacharda, M., 2003. Probable occurrence of sporadic permafrost in non-alpine scree slopes in central Europe. In: Phillips, M., Springman, S.M., Arenson, L.U. (Eds.), Proceedings of the 8th International Conference on Permafrost. Zurich, Switzerland, pp. 331–336.

Hauck, C., Kneisel, C., 2008. Quantifying the ice content in low-altitude scree slopes using geophysical methods. In: Hauck, C., Kneisel, C. (Eds.), Applied Geophysics in Periglacial Environments. Cambridge University Press, Cambridge, pp. 153–164.

Hauck, C., Vonder Mühll, D., 2003. Inversion and Interpretation of Two-dimensional Geoelectrical Measurements for Detecting Permafrost in Mountainous Regions. Permafr. Periglac. Process. 14, 305–318. https://doi.org/10.1002/ppp.462.

Jeník, J., 1961. Alpinská vegetace Krkonoš, Králického Sněžníku a Hrubého Jeseníku. Nakladatelství ČSAV, Praha.

Kneisel, C., 2010. The nature and dynamics of frozen ground in alpine and subarctic periglacial environments. The Holocene 20, 423–445. https://doi.org/10.1177/0959683609353432.

Kneisel, C., Hauck, C., 2008. Electrical methods. In: Hauck, C., Kneisel, C. (Eds.), Applied Geophysics in Periglacial Environments. Cambridge University Press, Cambridge, pp. 3–27.

Kneisel, C., Hauck, C., Vonder Mühll, D., 2000. Permafrost below the Timberline Confirmed and Characterized by Geoelectrical Resistivity Measurements, Bever Valley, Eastern Swiss Alps. Permafr. Periglac. Process. 11, 295–304. https://doi.org/10.1002/1099-1530(200012)11:4<295::AID-PPP353>3.0.CO;2-L.

Křížek, M., 2016. Periglacial landforms of the Hrubý Jeseník Mountains. In: Pánek, T., Hradecký, J. (Eds.), Landscapes and Landforms of the Czech Republic. Springer, Cham, pp. 277–289.

Lindgren, A., Hugelius, G., Kuhry, P., Christensen, T.R., Vandenberghe, J., 2016. GIS-based Maps and Area Estimates of Northern Hemisphere Permafrost Extent during the Last Glacial Maximum. Permafr. Periglac. Process. 27, 6–16. https://doi.org/10.1002/ppp.1851.

Morard, S., Delaloye, R., Dorthe, J., 2008. Seasonal thermal regime of a mid-latitude ventilated debris accumulation. In: Kane, D.L., Hinkel, K.M. (Eds.), Proceedings of the 9th International Conference on Permafrost. Fairbanks, Alaska, pp. 1233–1238.

Morard, S., Delaloye, R., Lambiel, C., 2010. Pluriannual thermal behavior of low elevation cold talus slopes in western Switzerland. Geogr. Helv. 65, 124–134. https://doi.org/10.5194/gh-65-124-2010.

Parkhomenko, E.I., 1967. Electrical Properties of Rocks. Plenum Press, New York.

Popescu, R., Vespremeanu-Stroe, A., Onaca, A., Vasile, M., Cruceru, N., Pop, O., 2017. Low-altitude permafrost research in an overcooled talus slope-rock glacier system in the Romanian Carpathians (Detunata Goală, Apuseni Mountains). Geomorphology 295, 840–854. https://doi.org/10.1016/j.geomorph.2017.07.029.

Růžička, V., Zacharda, M., Šmilauer, P., Kučera, T., 2015. Can paleorefugia of cold-adapted species in talus slopes resist global warming? Boreal Environ. Res. 20, 403–412.

Rybníček, K., Rybníčková, E., 2004. Pollen analyses of sediments from the summit of the Praděd range in the Hrubý Jeseník Mts (Eastern Sudetes). Preslia 76, 331–347.

Šafanda, J., Rajver, D., 2001. Signature of the last ice age in the present subsurface temperatures in the Czech Republic and Slovenia. Glob. Planet. Chang. 29, 241–257. https://doi.org/10.1016/S0921-8181(01)00093-5.

Schrott, L., Hoffmann, T., 2008. Refraction seismics. In: Hauck, C., Kneisel, C. (Eds.), Applied Geophysics in Periglacial Environments. Cambridge University Press, Cambridge, pp. 57–80.

Schrott, L., Sass, O., 2008. Application of field geophysics in geomorphology: advances and limitations exemplified by case studies. Geomorphology 93, 55–73. https://doi.org/10.1016/j.geomorph.2006.12.024.

Stan, D., Stan-Kłeczek, I., Kania, M., 2017. Geophysical approach to the study of a periglacial blockfield in a mountain area (Ztracené kameny, Eastern Sudetes, Czech Republic). Geomorphology 293, 380–390. https://doi.org/10.1016/j.geomorph.2016.12.004.

Stiegler, C., Rode, M., Sass, O., Otto, J.C., 2014. An Undercooled Scree Slope Detected by Geophysical Investigations in Sporadic Permafrost below 1000 M ASL, Central Austria. Permafr. Periglac. Process. 25, 194–207. https://doi.org/10.1002/ppp.1813.

Szewczyk, J., Nawrocki, J., 2011. Deep-seated relict permafrost in northeastern Poland. Boreas 40, 385–388. https://doi.org/10.1111/j.1502-3885.2011.00218.x.

Telford, W.M., Geldart, L.P., Sheriff, R.E., 1990. Applied Geophysics. Cambridge University Press, Cambridge.

Vandenberghe, J., French, H.M., Gorbunov, A., Marchenko, S., Velichko, A.A., Jin, H., Cui, Z., Zhang, T., Wan, X., 2014. The Last Permafrost Maximum (LPM) map of the Northern Hemisphere: permafrost extent and mean annual air temperatures, 25–17 ka BP. Boreas 43, 652–666. https://doi.org/10.1111/bor.12070.

Wicky, J., Hauck, C., 2017. Numerical modelling of convective heat transport by air flow in permafrost talus slopes. The Cryosphere 11, 1311–1325. https://doi.org/10.5194/tc-11-1311-2017.

Zacharda, M., Gude, M., Kraus, S., Hauck, C., Molenda, R., Růžička, V., 2005. The Relict Mite *Rhagidia gelida* (Acari, Rhagidiidae) as a Biological Cryoindicator of Periglacial Microclimate in European Highland Screes. Arct. Antarct. Alp. Res. 37, 402–408. https://doi.org/10.1657/1523-0430(2005)037[0402:TRMRGA]2.0.CO;2.

Zacharda, M., Gude, M., Růžička, V., 2007. Thermal Regime of Three Low Elevation Scree Slopes in Central Europe. Permafr. Periglac. Process. 18, 301–308. https://doi.org/10.1002/ppp.598.